THE ASTROPHYSICAL JOURNAL, 301:252–261, 1986 February 1

WZ SAGITTAE: TIME-RESOLVED SPECTROSCOPY DURING QUIESCENCE

RONALD L. GILLILAND
High Altitude Observatory, National Center for Atmospheric Research[1]

EDWARD KEMPER
Astronomy Programs, Computer Sciences Corporation

AND

NICHOLAS SUNTZEFF
Mount Wilson and Las Campanas Observatories, Carnegie Institution of Washington
Received 1985 February 8; accepted 1985 July 7

ABSTRACT

High time resolution spectroscopy has been used to obtain an orbital velocity amplitude for the primary component of the dwarf nova WZ Sagittae, an 82 minute binary, of $K_1 = 49 \pm 5$ km s^{-1}. The line profiles of Hα, some seven months after the 1978 December outburst of WZ Sge, were ideal for radial velocity determinations with the S-wave emission component being weaker than normal, while the system brightness was still above preoutburst levels. The higher orbital velocity yields standard solutions for the system masses of $M_1 \approx 1.1\ M_\odot$, $M_2 \approx 0.1\ M_\odot$. Implications of the new K_1 value and observed line profile variations for the physical model of WZ Sge are discussed. Relative phasing of the velocity and photometric eclipse does not agree with the canonical hot spot model. Si II absorption lines at 4130 and 3856–3863 Å redshifted at a stationary velocity of 270 km s^{-1} with respect to the systemic velocity of WZ Sge imply the existence of mass accretion to the system.

Subject headings: stars: dwarf novae — stars: eclipsing binaries — stars: individual

I. INTRODUCTION

WZ Sagittae was one of the first cataclysmic variables shown to be a binary system (Kraft 1961) from spectroscopic observations. Krzeminski (1962) found that WZ Sge was an eclipsing binary with an 81 minute 38 s orbital period. Krzeminski and Kraft (1964, hereafter KK), in the first of many comprehensive analyses of the WZ Sge system to appear in the literature, presented "a lower limit to certain detection of orbital velocity changes for the double emission feature is 2K = 75 km s^{-1}." Interpreted as an upper limit to K_1 of 37.5 km s^{-1}, this fundamental result has remained untested for two decades, although interpretations and observations of WZ Sge have led to a vast literature. Despite the lack of a well-determined orbital velocity, WZ Sge is one of the most thoroughly studied catalysmic variables. The ultrashort orbital period spurred several discussions of the astrophysical importance of gravitational radiation (Kraft, Mathews, and Greenstein 1962; Paczyński 1967; Faulkner 1971). The photometric properties during quiescence have been thoroughly studied and discussed (Krzeminski and Smak 1971; Warner and Nather 1972; Robinson, Nather, and Patterson 1978; Fabian *et al.* 1978; Ritter and Schroder 1979; Smak 1979; Patterson 1980), although a consensus concerning a unique set of model parameters has remained elusive.

WZ Sagittae was discovered as a nova in 1913 (Leavitt and Mackie 1919) and recognized as a recurrent nova with the discovery of its 1946 eruption (Mayall 1946), and reclassification as a dwarf nova was suggested (Warner 1976) based on spectroscopic properties. Its 1978 December outburst, discovered by J. T. McGraw (Patterson 1978), was closely followed and reported on by several groups. Outburst similarities to SU UMa supermaxima and the presence of superhumps led to several interpretations of these phenomena (Gilliland and Kemper 1980; Patterson *et al.* 1981; Leibowitz and Mazeh 1981). Extensive studies of WZ Sge have also been made in the ultraviolet with *IUE* during its recent outburst (Fabian *et al.* 1980; Holm *et al.* 1980; Friedjung 1981).

We present results of spectroscopic observations obtained seven months after the 1978 outburst of WZ Sge. The primary result is a substantial upward revision for the orbital velocity amplitude of the primary component. The higher velocity allows solutions for the component masses in which the secondary ($M_2 \approx 0.1\ M_\odot$) is resident on the zero-age main sequence while the white dwarf mass remains under the Chandrasekhar limit ($M_1 \approx 1.1\ M_\odot$). The phasing of radial velocities with the photometric eclipse suggest that the spot is on the opposite side of the disk from predictions of standard U Gem type models. We also find evidence for a substantial low-velocity mass inflow to the WZ Sge system.

II. OBSERVATIONS

On the night of 1979 July 16, we obtained time-resolved spectroscopy of WZ Sge over four orbital cycles with the ITS Cassegrain spectrograph (Miller, Robinson, and Schmidt 1980) on the 3 m Shane telescope of Lick Observatory. The 1200 line grating and red-sensitive image tube were used to provide optimal sensitivity and resolution at Hα. Continuum-source scans of incandescent lamps were taken before and after the observing sequence in order to flat-field the detector. Scans of a flux standard star (HD 182487) were obtained to allow reduction of the scans to an absolute flux calibration. Where trade-offs were necessary to obtain precise radial velocity information versus accurate flux calibration, all efforts were directed toward optimization for radial velocities. A narrow

[1] The National Center for Atmospheric Research is sponsored by the National Science Foundation.

entrance slit was used to obtain high resolution. Scans of comparison lamps were obtained after every third observation of the object to maintain precise wavelength calibrations. The standard procedure of alternatively observing sky and object in a 1/2-1-1/2 mode between two adjacent slits to obtain accurate sky subtraction was *not* followed. Again to optimize for radial velocity stability, long series of scans were obtained with the object remaining in the same slit. In general, sky background was not a problem, and even without balancing sky and object between the two slits, the background could be accurately removed (notice the lack of any [O I] night sky lines at 6300 and 6363 Å in Fig. 1 or Hg lines in Fig. 2).

In the red ($\sim$5750–7100 Å) we obtained 21 8 minute scans at a dispersion of 0.66 Å per channel, resulting in 2–3 Å resolution. These scans were obtained as two (12 and nine consecutive scans respectively) long time series (with different slits) separated by an interval of 2 hr. An additional set of seven 1 minute scans was obtained through an eclipse phase. Times of midexposure, orbital phase with respect to the Robinson, Nather, and Patterson (1978) ephemeris, radial velocities, and line strength and profile information for all scans are given in Table 1.

In the blue ($\sim$3800–5150 Å) we obtained 14 8 minute scans at a dispersion of 0.67 Å per channel, resulting in $\sim$3 Å resolution. A continuous series of 13 scans was obtained in one slit, with an additional scan obtained in the other slit. Somewhat later a series of 11 1 minute scans was obtained through an eclipse. Results are summarized in Table 1.

All scans were reduced with the following procedure: (1) Object and sky scans taken with the two slits were divided by the respective continuum scan to remove image tube response irregularities. (2) The sky background is subtracted from the object. (3) Using the procedures described in Stover *et al.* (1980) and Gilliland (1982*a*), the sky-subtracted scans were transformed to a uniform log λ scale. (4) Continuum was flattened by division by a fourth order polynomial for the red scans and a cubic for the blue scans. Care was taken to insure that the polynomial division neither obscured nor introduced any large-scale features into the resulting spectra. Sums based on 168 minutes for the red spectral region and 112 minutes for the blue are shown as Figures 1 and 2 respectively. Line identifications and line profile information are discussed in § IV.

III. RADIAL VELOCITIES

From examination of the comparison line scans taken after every third object scan, it was evident that no significant drift of wavelength versus position on the image tube face had occurred. The wavelength calibrations have relative precisions of $\lesssim 5$ km s^{-1} for the red scans near Hα and ~ 10 km s^{-1} for the blue scans from 4100 to 4900 Å. The calibration precisions are smaller than the precision with which the position of any spectral feature in WZ Sge can be measured; therefore final radial velocity errors are dominated by the ability to measure the position of given features. No attempts were made to calibrate with objects of known radial velocity; it is therefore possible, but unlikely, that the absolute velocity determinations could be in error by more than the above estimates.

The primary goal in planning the observations was to obtain precise relative radial velocities from analysis of the strong Hα emission feature. In the red scans only Hα was consistently strong enough to provide radial velocities. Signal-to-noise ratios (per pixel) near Hα are $\sim$20 for all 21 scans, with the intensity of the double emission varying from 2.5 to 3.5 times the continuum level. Several elements of the double Hα emission were analyzed for radial velocities: the central depression, the separate emission peaks, and the outer wings of the

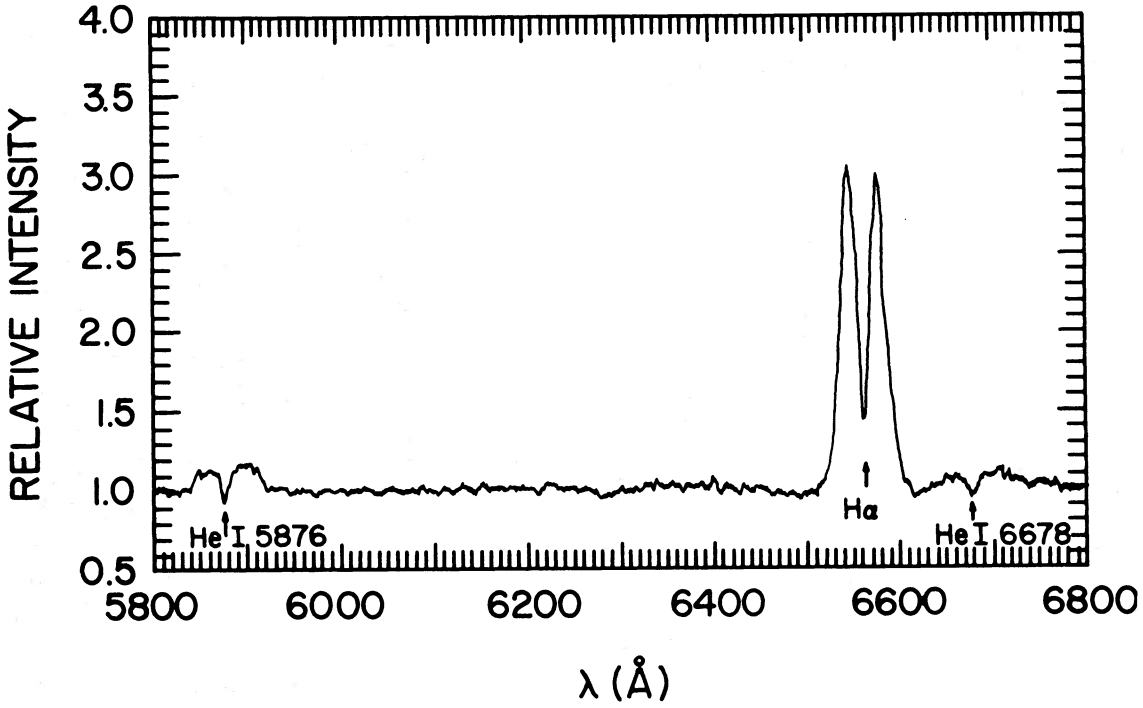

FIG. 1.—The sum of 21 8 minute scans of WZ Sge after shifting to a uniform wavelength scale and flattening the continuum with polynomial division

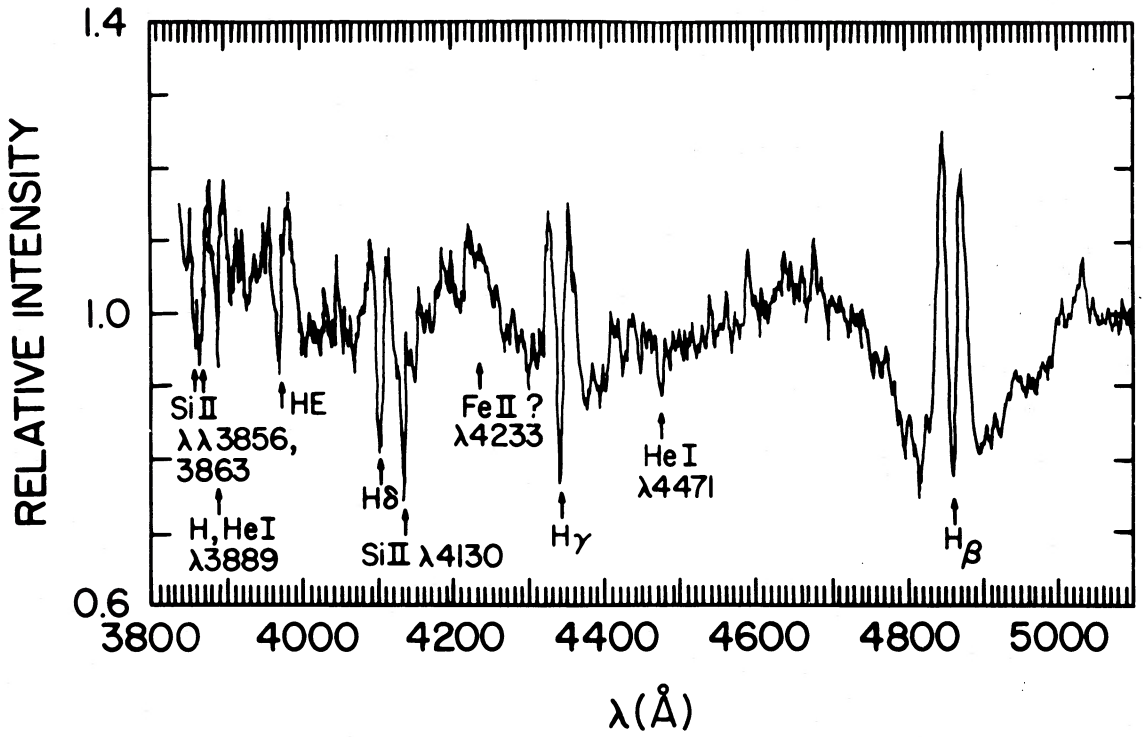

FIG. 2.—Same as Fig. 1, but for 14 8 minute blue scans

doubled emission. Analysis of the central trough yield velocities with large scatter and will not be further discussed.

The centroid of the doubled Hα feature was determined by fitting a three-parameter (height, position, and width) Gaussian profile to the outer wings with varying amounts of the central core weighted to zero. Radial velocity curves evaluated for different amounts of excluded core show systematic trends in the derived velocity amplitude and mean scatter. (See Shafter and Szkody 1984 for a discussion of similar behavior with an independent but similar analysis technique applied to T Leo.) Fitting only the outermost parts of the wings results in slightly smaller derived orbital amplitude with increased scatter and resultant errors. As points successively closer to the line core are included in the fit, the scatter about an orbital solution reaches a minimum at an excluded core width of 1700 km s^{-1} (the peaks have a mean separation of $\sim$1400 km s^{-1}). This solution is shown in Figure 3 and Table 2. The velocity amplitude is $K_1 = 48.2$ km s^{-1} with an rms scatter of 12.9 km s^{-1}. The optimal fit is thus obtained by fitting a Gaussian profile from 850 to 2000 km s^{-1} on each side of the line centroid. Reducing the excluded core to 1450 km s^{-1} resulted in $K_1 = 56.7$ km s^{-1} with a scatter of 15.8 km s^{-1}. The opposite extreme of excluding 2000 km s^{-1} from the core (starting fit $\sim$40% below peaks) yields $K_1 = 41.1$ km s^{-1} with a scatter of

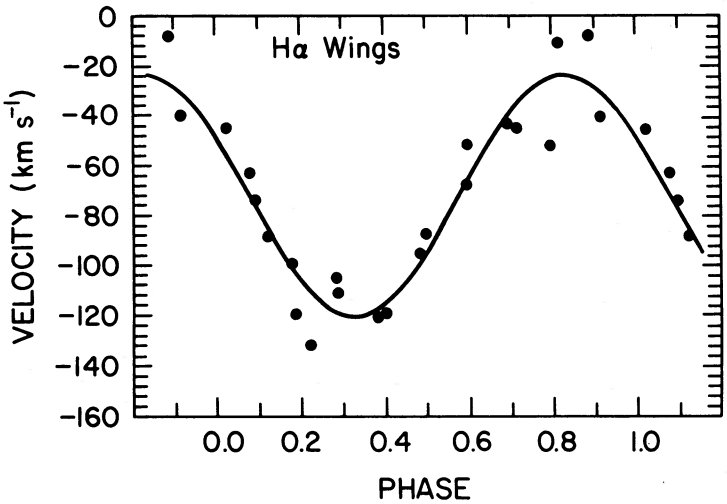

FIG. 3.—Radial velocity curve for WZ Sge. $\epsilon = 0$ is assumed, as well as the Robinson, Nather, and Patterson 1978 ephemeris. Velocities are for the wings of Hα.

TABLE 1

SPECTROSCOPIC OBSERVATIONS OF WZ SAGITTAE

HJD (2,444,070.+)	Exposure (minutes)	ϕ	Velocity (km s^{-1})	Equivalent Width (Å)	V/R
		Hα			
1.768	8	0.091	−74.3	89.8	1.084
1.773	8	0.190	−120.2	92.3	1.023
1.779	8	0.288	−111.8	95.4	1.175
1.785	8	0.401	−119.7	96.6	1.028
1.791	8	0.500	−87.7	97.0	1.040
1.797	8	0.599	−52.0	102.0	0.934
1.803	8	0.718	−45.3	93.7	0.967
1.809	8	0.817	−11.2	89.3	0.922
1.814	8	0.916	−40.2	95.1	0.868
1.821	8	0.026	−45.5	98.2	0.957
1.826	8	0.124	−88.3	98.6	0.943
1.832	8	0.223	−132.3	103.4	1.043
1.926	8	0.890	−8.4	62.1	0.963
1.937	8	0.080	−63.4	72.8	0.993
1.943	8	0.179	−100.4	79.6	1.020
1.949	8	0.288	−105.4	83.8	1.057
1.955	8	0.387	−120.8	89.4	1.121
1.960	8	0.485	−95.6	84.3	1.027
1.967	8	0.598	−67.6	77.3	1.000
1.972	8	0.697	−44.3	58.7	1.027
1.978	8	0.796	−52.5	60.5	1.004
1.930	1	0.946	...	57.3	0.993
1.930	1	0.959	...	60.8	1.055
1.931	1	0.972	...	66.2	1.214
1.932	1	0.985	...	76.4	1.182
1.933	1	0.998	...	79.6	0.906
1.933	1	0.011	...	77.1	1.041
1.934	1	0.024	...	76.1	0.944
		Hβ			
1.839	8	0.351	−231.8	48.3	1.072
1.845	8	0.450	−178.1	43.6	1.055
1.852	8	0.569	−149.5	43.1	1.098
1.857	8	0.668	−143.5	39.0	1.101
1.863	8	0.767	−130.6	32.8	1.089
1.869	8	0.878	−56.3	29.1	0.914
1.875	8	0.977	−118.8	28.7	0.967
1.880	8	0.076	−63.6	28.4	1.009
1.887	8	0.186	−238.4	23.7	0.844
1.892	8	0.285	−224.1	24.1	1.000
1.898	8	0.384	−201.3	22.6	1.088
1.904	8	0.493	−147.0	30.3	0.991
1.909	8	0.592	−188.4	34.5	1.018
1.916	1	0.708	...	27.8	1.079
1.984	1	0.913	...	39.4	0.927
1.985	1	0.926	...	41.2	0.780
1.986	1	0.939	...	32.7	0.944
1.987	1	0.952	...	31.8	0.919
1.987	1	0.965	...	33.6	0.982
1.988	1	0.978	...	39.3	0.951
1.989	1	0.991	...	40.2	0.982
1.990	1	0.004	...	38.9	0.950
1.990	1	0.017	...	38.2	0.893
1.991	1	0.031	...	28.3	1.000
1.992	1	0.043	...	31.3	1.009

19.2 km s^{-1}. The latter trend is expected; fitting farther out in the wings (and thus discarding most of the velocity information) should lead to smaller derived amplitudes with increased scatter. The formal 1 σ error on the optimal fit is 4 km s^{-1}; allowance for a possible systematic effect associated with different definitions of the line core results in a velocity amplitude of 48 ± 6 km s^{-1}. The analyses with different core definitions all gave consistent phases for maximum recessional

TABLE 2

RADIAL VELOCITY FITS[a] FOR WZ SAGITTAE

Line	K (km s^{-1})	γ (km s^{-1})	ω (2π rad)	σ_{SD}
Hα wings	48. ± 4.	−72. ± 3.	0.83 ± 0.01	12.9
Hα red peak	42. ± 14.	+630. ± 10.	0.77 ± 0.05	45.0
Hα blue peak	41. ± 12.	−748. ± 9.	0.86 ± 0.05	39.7
Hβ wings	63. ± 16.	−149. ± 12.	0.86 ± 0.04	40.2
λ4133	8. ± 12.		0.86 ± 0.27	33.4

[a] Assumes $\epsilon = 0$ and the Robinson, Nather, and Patterson 1978 ephemeris.

velocity and were consistent with circular orbits. The optimal case discussed above, reduced without assuming a circular orbit, produced $K_1 = 48.7$ km s^{-1}, $\epsilon = 0.10 \pm 0.09$. *We believe the quoted velocity amplitude of* 48 ± 6 km s^{-1} *reasonably reflects the best solution and possible associated errors, but that systematic errors of the type discussed above are more likely to have resulted in too small an estimate, rather than too large.*

In Figure 4 the resulting velocities and circular orbital fits are shown for the two peak components separately. The blue component shows $K = 41$ km s^{-1}, $\gamma' = -748$ km s^{-1}, $\omega = 0.86$, and $\sigma = 40$ km s^{-1}, while the red component shows $K = 42$ km s^{-1}, $\gamma' = 630$ km s^{-1}, $\omega = 0.77$, and $\sigma = 45$ km s^{-1}, Two interesting results are evident from Figure 4: (1) The blue component shows anomalous positive velocities at $\phi = 0.7$–0.8, while the red component shows anomalous negative velocities at $\phi \approx 0.2$. These excursions are quite readily explained by the interference of the S-wave emission component (KK) with the individual peaks, *if the velocity amplitude of the S-wave is smaller than half the peak separation.* (We note that the V/R variations discussed below and shown in Fig. 6 for Hα suggest that the extra emission component arises from the disk side opposite the secondary and thus could not influence the peaks as noted here.) An S-wave component with a velocity amplitude carrying it outside the doubled peaks would create velocity anomalies at the same phases as observed, but of opposite sign. Since the S-wave remained within the peaks, it should not adversely bias velocity estimates based on the outer wings. (The S-wave was also weaker during our observations than had been reported in earlier studies, e.g., KK). (2) Outside of the anomalous velocities at $\phi = 0.2$, 0.7 as noted above, the peaks show (by inspection) orbital velocities well below 40 km s^{-1}. This is essentially the method used by KK to set a limit on the orbital velocity, and consistent results are obtained. We may therefore conclude that KK were correct in saying that the peaks were stationary to a limit of $2K < 75$ km s^{-1}, their limit for certain detection. We have, however, claimed above that $K = 48 \pm 6$ km s^{-1}, based on analysis of the line wings. Which result should be accepted as the *real* orbital velocity?

Adopting the standard approach, we could readily claim that the velocity obtained from analysis of the wings is correct, since nearly all recent studies of velocities of emission lines in cataclysmic variables have assumed this. This quite reasonable and probably correct assumption is based on the following reasoning. The outer line wings are formed by emission processes occurring in material in Keplerian motion close to the white dwarf. This high-velocity material is deep in the uniform potential well of the white dwarf. The emission peaks, however, are formed by lower velocity material farther out in the disk and are thus from a less circular distribution of gravitational

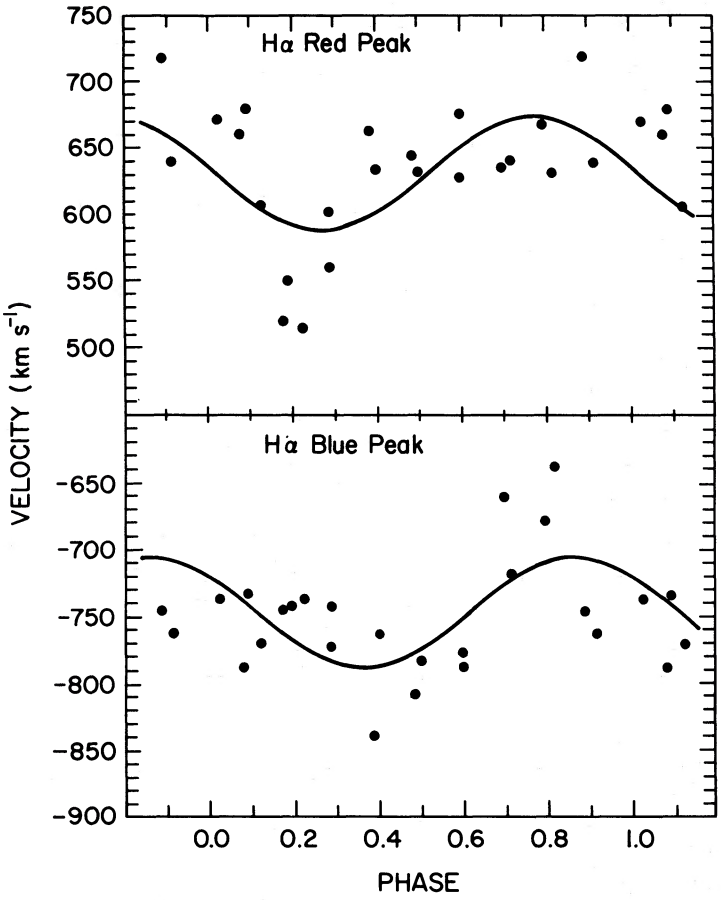

FIG. 4.—Radial velocity curves for the (*bottom*) blue and (*top*) red Hα peaks. $\epsilon = 0$ is assumed, as well as the Robinson, Nather, and Patterson 1978 ephemeris.

potential. Furthermore, the outer regions of the disk directly suffer the disturbance of an impacting accretion stream leading to the S-wave. It is certainly simplest and reasonable to assume that the velocity of the primary is best evidenced by the material closest to it. The discrepancies between the velocities presented in Figures 3 and 4 are evidence of significant nonuniformities at least in the outer disk.

We have analyzed the wings of the Hβ emission with the same procedure followed for Hα. The result is of much lower significance due to several problems: (1) lower velocity resolution at Hβ than Hα, (2) fewer comparison lines in the blue, (3) lower signal-to-noise ratio in the blue, (4) weaker emission at Hβ, (5) strong, perhaps variable, underlying absorption at Hβ, and (6) fewer scans. The resulting velocity is $K_1 = 63 \pm 16$ km s^{-1}, $\omega = 0.86$, $\gamma = -149$ km s^{-1}, and $\sigma = 40$ km s^{-1}. We adopt $K_1 = 49 \pm 6$ km s^{-1} as the final estimate of the orbital velocity amplitude. Table 2 summarizes the radial velocity results. (While the radial velocities of Hα and Hβ are in agreement, they show quite different behavior in terms of V/R; see Figs. 6 and 7.)

The only other feature consistently strong enough for velocity measurements is the sharp absorption feature at ~4133 Å (to be further discussed in the next section). The radial velocities for this feature, assuming $\lambda = 4133$ Å, are shown in Figure 5 and summarized in Table 2. The resulting amplitude is $K = 8 \pm 12$ km s^{-1}, a result consistent with no variation but inconsistent with the adopted orbital variation of 49 km s^{-1}.

IV. LINE VARIATIONS AND PROPERTIES

a) General Description of the Spectrum

The red scan, as shown in Figure 1, is dominated by the doubled emission line of Hα. There is no evidence of any broad underlying absorption, and any such feature must have a depth of less than 10%. Doubled He I lines at 5876 and 6678 Å are present, both having central absorption below the continuum level. No other lines are present in the red scan.

The blue scan (see Fig. 2) is much more complex. Hβ and the higher order Balmer lines show very broad (full width >300 Å at Hβ) absorption features, as noted by Greenstein (1957), who attributed these to white dwarf lines. Robinson, Nather, and Patterson (1978) argued that the broad absorption was formed in the accretion disk, while Smak (1979) and Patterson (1980) tend to support formation on the white dwarf. (The broad absorption features cannot be measured for radial velocities with precisions required to yield K_1.) The Balmer lines all show doubled emission. He I λ4471 is weakly present as an absorption core and shows doubled emission in some individual scans. He II λ4686 and C III–N III λ4650 are not identifiable. The strongest absorption feature in the spectrum is at 4133 Å and is unexpected. A broad emission feature occurs near 4233 Å and may be attributable to Fe II emission.

b) Variations of Hα *and* Hβ

The equivalent widths (EW) and ratio of violet to red (V/R) peak heights for Hα are listed in Table 1 and shown in Figure

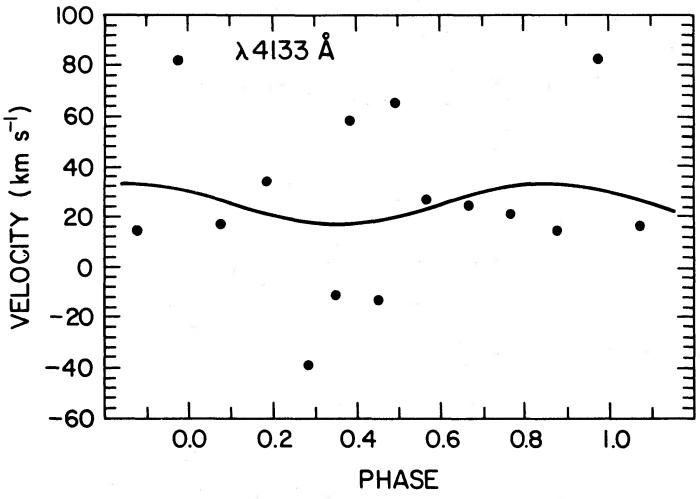

FIG. 5.—Radial velocity curve for the λ4133 feature

6. Over the two disjoint observing periods in the red, the EW of Hα showed quite different behavior. In the first run the EW showed very little variation over the orbital cycle and had a mean value of 96.0 ± 4.4 Å. Two hours later the EW showed a very significant orbital variation of half-amplitude 13.9 ± 1.5 Å, peaking at $\phi = 0.34 \pm 0.01$, with a mean value of 74.1 Å. Through eclipse the EW reach a local maximum at $\phi \approx 0.0$, presumably the result of suppressed continuum. Although the EW showed quite different behavior during the two periods, the radial velocities showed no differences—suggesting that systematic velocity errors as a function of line strength are not important. The V/R show small but consistent variation with orbital phase with half-amplitude of 0.06 ± 0.02, mean $= 1.01 \pm 0.01$, and maximum at $\phi = 0.34 \pm 0.04$, shown in Figure 6. This does not fit the canonical model, in which maximum V/R occurs at $\phi \approx 0.6$–0.7 as the hot spot is

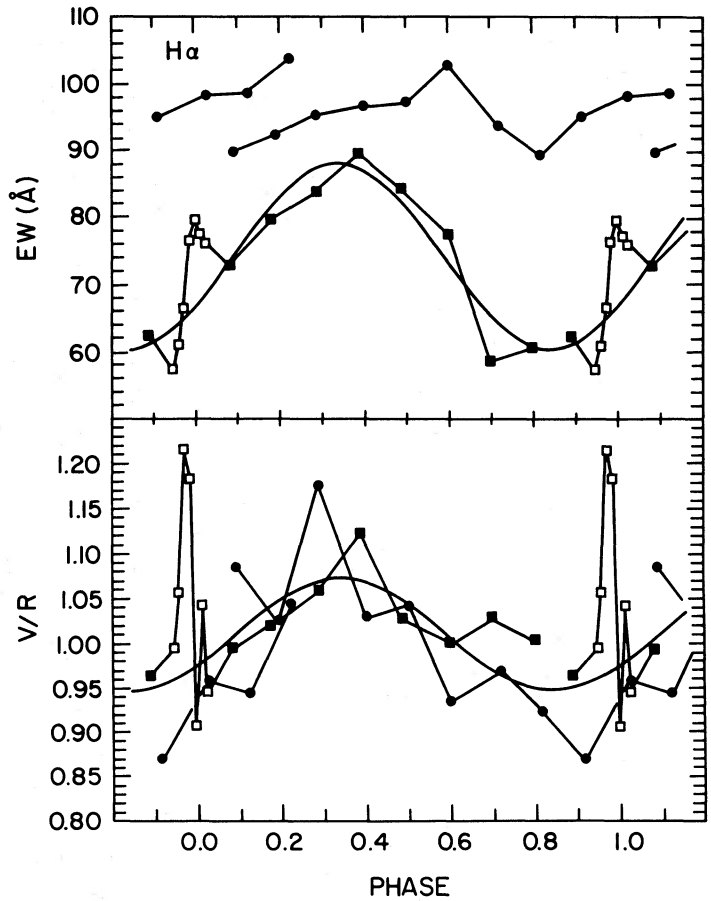

FIG. 6.—(*top*) The equivalent widths and (*bottom*) the V/R ratio for the doubled Hα emission. Contiguous points in time are connected and open symbols are from 1 minute scans.

approaching the observer (see, e.g., Fig. 4 of Gilliland 1982*b* for V/R in EX Hya). We return to this discrepancy in the next section. During the phases near eclipse, the series of 1 minute scans shows a narrow maximum of V/R at $\phi = 0.97$–0.98.

The EW and V/R for Hβ are shown in Figure 7 and listed in Table 1. The 1 minute scans near eclipse were obtained 2 hr after the other series. Measurement errors are much more serious for Hβ than for Hα due to lower signal-to-noise ratio and the complication of strong underlying absorption. The EW show a weak orbital dependence with half-amplitude $= 5.5 \pm 2.1$ Å, mean $= 31.5 \pm 1.5$ Å, peaking at $\phi = 0.56 \pm 0.06$. The EW through eclipse (very noisy data) suggest maxima at $\phi \approx 0.92$ and ~ 0.99. V/R for Hβ show an orbital variation of half-amplitude $= 0.07 \pm 0.02$, mean $= 1.01 \pm 0.01$, peaking at $\phi = 0.58 \pm 0.04$.

c) λ4133 *Absorption Feature*

As discussed in § III, this feature shows a stationary velocity. With respect to the rest frame of WZ Sge ($\gamma = -72$ km s^{-1} from Hα), the line is at a wavelength of 4133.4 ± 1.0 Å. It varies in strength from a core residual intensity of 0.6 of continuum to greater than 0.9 with a mean of 0.73. The equivalent width is 1.5 ± 0.2 Å, the variations having no correlation with orbital phase. The line is undoubtedly real, consistently present in the WZ Sge blue scans, with no corresponding feature in either the blue comparison star scans or the red WZ Sge scans, as might be expected if this were a tube glitch. The most likely identification is with a Si II doublet with a mean wavelength of 4129.6 Å commonly seen in shell-star spectra (Broyles 1943; Heap 1976). At our dispersion the doublet should not be resolved. If this is the correct identification, one might expect to see another pair of Si II lines at 3856, 3863 Å, which should be marginally resolved at our resolution. Indeed, just inside the blue limit of our scans, there is just such a doubled absorption feature at just the right wavelengths to support the assertion that these lines are due to Si II.

Despite the wavelength coincidences, the identification of these features is not ironclad. The Si II doublet near 4130 Å arises from about 9.8 V above the ground state of the ion (Moore 1965). The lines near 3860 Å arise from a level at ~ 6.9 V. (No evidence of lines at 6347 and 6371 Å arising from an intermediate excitation potential of 8.1 V are seen. We do not have an explanation for the absence of these lines if the observed features are Si II.) These high-excitation lines are presumably being produced in material which is outside the system at some distance from the high-energy events which might provide the photons or the kinetic energy needed to populate the energy levels involved. Furthermore, the ultraviolet lines near 2072 Å which come from the same lower level as the doublet near 3860 Å were not observed during outburst (Fabian *et al.* 1980). The same is true for the UV lines near 2905 Å which arise from the same level as the 4130 Å doublet (Fabian *et al.* 1980). Thus further work is needed to identify securely these "Si II" features.

The absoption feature at 4133 Å, interpreted as Si II, implies the existence of material outside the system with an *infall* veloc-

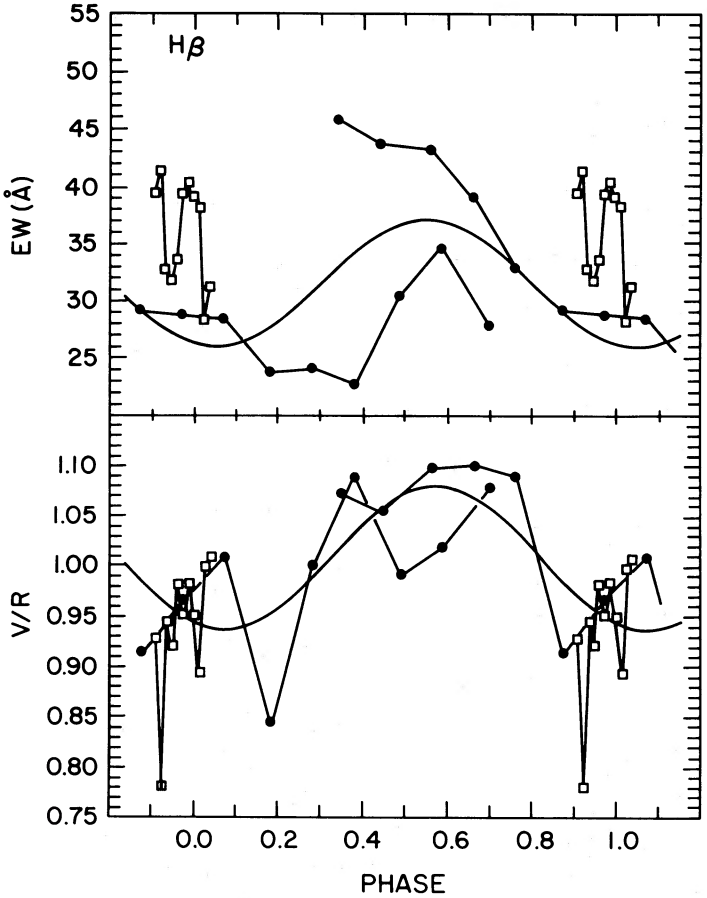

FIG. 7.—Same as Fig. 6, but for Hβ

ity of 270 ± 70 km s^{-1}. Immediately following the outburst, seven months before these observations, material was outside the system in WZ Sge (Gilliland and Kemper 1980; Brosch, Leibowitz, and Mazeh 1980). (Voikhanskaya 1983 has presented independent evidence for the existence of circumstellar material in WZ Sge.) This material was probably expelled at moderate velocities, some of it collecting to form an external disk with an orbital velocity of ~220 km s^{-1} (Gilliland and Kemper 1980; Leibowitz and Mazeh 1981). We note that the infall velocity is just less than the free-fall velocity at the radius of the external disk. Could it be that the WZ Sge system is accreting material, either from the interstellar medium or ejected during the previous outburst, that becomes dense enough to form an absorption feature when at the radius of the previously established external disk?

V. INTERPRETATION

a) System Masses

The wings of Hα can be traced out to a velocity of 2400 km s^{-1} from line center. Interpreted as Keplerian velocities in the inner disk and using the Shipman (1977) mass-radius relation for white dwarfs, this places a lower limit to the primary mass of $M_{WD} > 0.44\ M_\odot$. This is a nontrivial limit, since many recent studies have considered masses smaller than this (Robinson, Nather, and Patterson 1978; Fabian *et al.* 1978; Smak 1979).

A canonical approach to estimating masses in cataclysmic variables is to use the assumption that the secondary is precisely filling its Roche lobe, thus allowing a calculation of its mean density (Faulkner 1971). Then with knowledge of a mass-radius relation for an assumed secondary star type (usually zero-age main sequence), one directly obtains a secondary mass. Use of the mass function from the radial velocity analysis, with constraints on the orbital inclination, then allows one to solve for the primary mass. This technique has been avoided with WZ Sge, since its application for $K_1 < 38$ km s^{-1} (KK) invariably leads to white dwarf masses well above the Chandrasekhar limit.

The higher value for K_1 of 49 km s^{-1} implies that the estimated primary mass will be smaller for a given, assumed secondary mass. Rappaport, Joss, and Webbink (1982) have argued that mass loss on shorter than thermal time scales can lead to distended radii and thus a smaller mass than that derived using standard mass-radius relations. Adopting the Lacy (1977) mass-radius relation for lower main-sequence stars and allowing for mildly distended radii a secondary mass of about 0.1 $M_\odot$ is reasonable. Assuming an orbital inclination of 80°, the above secondary mass, and the adopted orbital solution leads to $M_{WD} \approx 1.1\ M_\odot$. The "canonical" approach can therefore yield a large but physically reasonable value for the primary mass. We should, however, stress that the estimate of the secondary mass is uncertain at least to the 25% level, which would allow solutions for the white dwarf mass in conflict with the Chandrasekhar limit.

Are the results $M_2 = 0.1\ M_\odot, M_{WD} = 1.1\ M_\odot$ consistent with the recent analyses of eclipse profiles for WZ Sge (Fabian *et al.* 1978; Ritter and Schroder 1979)? Interpolation in Figure 2 of Fabian *et al.* (1978) for $K_1 = 49$ km s^{-1} suggests possible solutions with $q, i = (11, 69°)$ to $q, i = (7, 78°)$. Similarly, from Figure 5 of Ritter and Schroder (1979), possible solutions (constrained by lines 2 and 3) are $q, i = (8, 77°)$ to $q, i = (6.3, 77°)$. With both sets of constraints we must have $q, i = (7–8, 77°)$ for $K_1 = 49$ km s^{-1}. With the derived mass function of $f(M_\odot) = 6.67 \times 10^{-4}$, we have $M_2 = 0.05–0.06$ and $M_{WD} = 0.37–0.49$. But with $i = 77°$, the observed line width of Hα at zero intensity requires $M_{WD} > 0.45\ M_\odot$. If we use constraint 1 of Ritter and Schroder (1979) and choose $i = 75°$, then $q = 10.6$ is required with $K_1 = 49$ km s^{-1}; this is satisfied with $M_2 = 0.1\ M_\odot$ and $M_{WD} = 1.06\ M_\odot$, essentially the result suggested above for the "canonical" assumptions.

We thus arrive at estimates for the system parameters with possible values of q from 8 to 11, $i \approx 75–77°$, $M_2 \approx 0.06–0.11\ M_\odot$, and $M_{WD} \approx 0.5–1.2\ M_\odot$. We note that if $M_2 \approx 0.06\ M_\odot$, $M_{WD} \approx 0.5\ M_\odot$ the secondary is degenerate and the orbital period should be increasing; if $M_2 \approx 0.1\ M_\odot$, $M_{WD} \approx 1.1\ M_\odot$ the secondary is still nondegenerate with orbital evolution toward decreasing periods. Since Robinson, Nather, and Patterson (1978) were unable to detect a period change based on data over nearly half an outburst period, observational discrimination based on period changes between the high- and low-mass solutions seems only a remote possibility.

b) Problems with the System Geometry

One severe problem encountered in the radial velocity analyses (*if interpreted in terms of the standard hot spot model*) is the phase of peak recessional velocity, $\omega = 0.83 \pm 0.01$. From the photometric properties at quiescence (Robinson, Nather, and Patterson 1978), the expected maximum velocity occurs at $\omega = 0.71 \pm 0.02$, a discrepancy of 45 ± 10°. This cannot be explained by phase slippage following the outburst—we had simultaneous photometry verifying the preoutburst ephemeris (see also Patterson *et al.* 1981). Two possible explanations arise, neither of which seems entirely satisfactory: (1) The standard hot spot eclipse model is wrong. Instead the eclipse is of a feature on the opposite disk edge (perhaps part of a spiral dissipation pattern, suggested by Lin and Papaloizou 1979, or wind-induced hot spot, as suggested by Shafter and Szkody 1984). This would yield consistent eclipse and radial velocity phases. It should be noted that the canonical model of WZ Sge was developed by Krzeminski and Smak (1971) based on the photometric eclipses and S-wave radial velocities. The S-wave velocities may not be representative of Keplerian motion in the disk, due to stream impact effects. Krzeminski and Smak (1971) used the framework developed for U Gem, in which the light curve shows a hump immediately preceding the eclipse, even though the highly variable WZ Sge light curve only sometimes resembled that of U Gem. The velocity measures discussed in this paper are a more fundamental indication of the system geometry. (2) Distortions of the inner disk in Keplerian motion at velocities $\gtrsim 1000$ km s^{-1} are great enough to yield a phase shift of 45°. This seems most unlikely since: (*a*) the wings of Hα had a clean, symmetric appearance; (*b*) a circular orbit solution worked well; (*c*) V/R variations are not large; (*d*) the velocities seem not to be affected by substantial equivalent width changes; (*e*) varying the portion of the line wings in the least-squares fits did not lead to changes in ω; and (*f*) we have argued that the S-wave did not influence the wings. All of the above suggest that the radial velocity determinations are in fact correct.

A curious coincidence(?) arises if we recall the velocity analyses obtained immediately following the 1978 December outburst of WZ Sge. Walker and Bell (1980) detected a radial velocity variation of the absorption features during outburst with $K = 160$ km s^{-1} and $\omega = 0.84 \pm 0.03$ and atttributed this to the orbital velocity of the primary. Walker and Bell predict-

ed that observations of the double emission lines with modern detectors would show an orbital variation of $K_1 = 160$ km s^{-1}; this assertion we have disproven. Gilliland and Kemper (1980) also studied the absorption line velocity variations during outburst and found $K = 145$ km s^{-1}, $\omega = 0.836 \pm 0.01$, but did not attribute this to orbital variations of the primary, since it was a factor of 4 in conflict with the KK upper limit and had an unexpected phase. In this study we have determined the orbital motion of the primary to be $K_1 = 49$ km s^{-1}, $\omega = 0.834 \pm 0.01$. Why, if the radial velocities detected during outburst in absorption features were not indicative of orbital motion, do the phases of velocities after outburst in emission features agree perfectly within the allowed errors? (There is less than a 1% chance of mere coincidence.)

Another problem with the canonical hot spot model involves the phases of the V/R variations for Hα shown in Figure 6. Maximum V/R occurs at $\phi = 0.34$, while the S-wave interfering with a constant double-peaked profile maximize V/R at $\phi \approx 0.7$. It appears that the V/R ratios are more influenced by something on the opposite side of the disk from the hot spot than by the hot spot itself.

Although in disagreement with the basic conclusion of Walker and Bell (1980) concerning the orbital velocity amplitude, we are in reluctant agreement that the evidence "indicates that the source eclipsed at minimum light lies on the side of the line of centers of the two stars opposite the S-wave emission." We are therefore inclined to regard with skepticism all the system parameters based on analysis of eclipse timings, since a basic underlying assumption concerning the location of the eclipsed region may be incorrect. Similar effects have been seen in HT Cas (Young, Schneider, and Shectman 1981) and T Leo (Shafter and Szkody 1984); the latter discusses several potential explanations of this phenomenon. The most attractive mechanism involves a wind from the secondary which interacts most strongly with a region of the disk close to the secondary with a large velocity component into the wind. This would produce shock-induced heating in a location qualitatively consistent with the observations. It might prove fruitful to further study WZ Sge over the course of its 33 yr time scale between outbursts. Will the canonical hot spot model once again be appropriate for the prototypical cataclysmic variable if the S-wave component strengthens to its preoutburst level?

VI. CONCLUSIONS

We have detected an orbital velocity variation for the primary in WZ Sge of $K_1 = 49 \pm 6$ km s^{-1}. The new orbital solution yields masses of $M_{WD} = 1.1\ M_\odot$, $M_2 = 0.1\ M_\odot$, assuming the secondary to be resident on the main sequence. Solutions with masses up to a factor of 2 below the above estimates in which the secondary is now degenerate and the minimum orbital period has been passed are also possible. Uncertainty in the secondary mass also allows solutions with M_{WD} above the Chandrasekhar limit. Phasing of the orbital velocities with respect to eclipses suggests that the photometric eclipses are of the leading edge of the disk—opposite the canonical S-wave emission source. Thus WZ Sge, one of the first cataclysmic variables conclusively demonstrated to be a binary system and intensively studied over decades, *does not fit the canonical hot spot model.* A strong stationary absorption feature at 4133 Å tentatively identified with Si II λ4130 suggests accreting material at a velocity of 270 km s^{-1}.

This paper has raised two problems without providing adequate resolution (phasing of radial velocities and absorption feature at 4133 Å). The observed phasing of radial velocities with photometric eclipses is an extremely bothersome point, observed in both outburst and quiescence, which calls into question a standard interpretive construct often used in discussing catalysmic variables. It is the hope of the authors that raising these specific issues will spur others to further analyze unpublished data collected during the 1978 outburst of WZ Sge and perhaps to initiate new studies directed at these problems.

We thank J. Faulkner for assisting with obtaining the observations. We acknowledge interesting discussions with J. Faulkner, R. P. Kraft, M. F. Walker, and A. Young. A. Young also provided useful comments on the manuscript. We also thank an anonymous referee for thoughtful comments.

REFERENCES

Brosch, N., Leibowitz, E. M., and Mazeh, T. 1980, *Ap. J. (Letters)*, **236**, L29.
Broyles, A. A. 1943, *Ap. J.*, **97**, 234.
Fabian, A. C., Lin, D. N. C., Papaloizou, J., Pringle, J. E., and Whelan, J. A. J. 1978, *M.N.R.A.S.*, **184**, 835.
Fabian, A. C., Pringle, J. E., Stickland, D. J., and Whelan, J. A. J. 1980, *M.N.R.A.S.*, **191**, 457.
Faulkner, J. 1971, *Ap. J. (Letters)*, **170**, L99.
Friedjung, M. 1981, *Astr. Ap.*, **99**, 226.
Gilliland, R. L. 1982*a*, *Ap. J.*, **261**, 617.
———. 1982*b*, *Ap. J.*, **258**, 576.
Gilliland, R. L., and Kemper, E. 1980, *Ap. J.*, **236**, 854.
Greenstein, J. L. 1957, *Ap. J.*, **126**, 23.
Heap, S. R. 1976, in *IAU Symposium 70, Be and Shell Stars*, ed. A. Slettebak (Dordrecht: Reidel), p. 315.
Holm, A. U., Wu, C. C., Sparks, W. M., Schiffer, F. H., III, and Bogess, A. 1980, in *IAU Symposium 88, Close Binary Stars: Observations and Interpretations*, ed. M. Plavec, D. Popper, and R. Ulrich (Dordrecht: Reidel), p. 447.
Kraft, R. P. 1961, *Science*, **134**, 1433.
Kraft, R. P., Mathews, J., and Greenstein, J. L. 1962, *Ap. J. (Letters)*, **136**, 312.
Krzeminski, W. 1962, *Pub. A.S.P.*, **74**, 66.
Krzeminski, W., and Kraft, R. P. 1964, *Ap. J.*, **140**, 921 (KK).
Krzeminski, W., and Smak, J. 1971, *Acta Astr.*, **21**, 133.
Lacy, C. H. 1977, *Ap. J. Suppl.*, **34**, 479.
Leavitt, H. S., and Mackie, J. C. 1919, *Harvard Circ.*, No. 219.
Leibowitz, E. M., and Mazeh, T. 1981, *Ap. J.*, **251**, 214.
Lin, D. N. C., and Papaloizou, J. 1979, *M.N.R.A.S.*, **186**, 799.
Mayall, M. W. 1946, *Harvard Bull.*, No. **918**, p. 3.
Miller, J. S., Robinson, L. B., and Schmidt, G. D. 1980, *Pub. A.S.P.*, **92**, 702.
Moore, C. E. 1965, *Selected Tables of Atomic Spectra* Si II, Si III, Si IV (NSRDS-NBS 3, Sec. 1).
Paczyński, B. 1967, *Acta Astr.*, **17**, 287.
Patterson, J. 1978, *IAU Circ.*, No. 3311.
———. 1980, *Ap. J.*, **241**, 235.
Patterson, J., McGraw, J. T., Colman, L., and Africano, J. L. 1981, *Ap. J.*, **248**, 1067.
Rappaport, S., Joss, P. C., and Webbink, R. F. 1982, *Ap. J.*, **254**, 616.
Ritter, H., and Schroder, R. 1979, *Astr. Ap.*, **76**, 168.
Robinson, E. L., Nather, R. E., and Patterson, J. 1978, *Ap. J.*, **219**, 168.
Shafter, A. W., and Szkody, P. 1984, *Ap. J.*, **276**, 305.
Shipman, H. L. 1977, *Ap. J.*, **213**, 138.

Smak, J. 1979, *Acta Astr.*, **29**, 325.
Stover, R. J., Robinson, E. L., Nather, R. E., and Montemayor, T. J. 1980, *Ap. J.*, **240**, 597.
Voikhanskaya, N. F. 1983, *Sov. Astron.*, **27**, 541.
Walker, M. F., and Bell, M. 1980, *Ap. J.*, **237**, 89.
Warner, B. 1976, in *IAU Symposium 73, The Structure and Evolution of Close Binary Systems*, ed. P. Eggleton, S. Mitton, and J. Whelan (Dordrecht: Reidel), p. 85.
Warner, B., and Nather, R. E. 1972, *M.N.R.A.S.*, **156**, 297.
Young, P., Schneider, D. P., and Shectman, S. A. 1981, *Ap. J.*, **245**, 1035.

RONALD L. GILLILAND: High Altitude Observatory/NCAR, P.O. Box 3000, Boulder, CO 80307

EDWARD KEMPLER: Astronomy Programs, Computer Sciences Corporation, Space Telescope Science Institute, Homewood Campus, Baltimore, MD 21218

NICHOLAS SUNTZEFF: Mt. Wilson and Las Campanas Observatories, Carnegie Institution of Washington, 813 Santa Barbara Street, Pasadena, CA 91101